Sensors and Materials, Vol. 33, No. 6 (2021) 2227–2234
MYU Tokyo

S & M 2611

Near-infrared Phosphors: Photophysical Properties of Calcium-doped YSGG:Cr^{4+}

Takayuki Nakanishi,[1*] Makoto Tsurui,[2] Jian Xu,[3]
Nao Takahashi,[4] Takashi Takeda,[1] and Naoto Hirosaki[1]

[1]Research Center for Functional Materials, National Institute for Materials Science,
1-1 Namiki, Tsukuba, Ibaraki 305-0044, Japan
[2]Graduate School of Chemical Sciences and Engineering, Hokkaido University,
N 13, W 8, Kita-ku, Sapporo, Hokkaido 060-8628, Japan
[3]International Center for Young Scientists (ICYS), National Institute for Materials Science,
1-1 Namiki, Tsukuba, Ibaraki 305-0044, Japan
[4]Department of Materials Science and Technology, Tokyo University of Science,
6-3-1 Niijuku, Katsushika-ku, Tokyo 125-8585, Japan

(Received January 30, 2021; accepted May 10, 2021)

Keywords: garnet, near-infrared, chromium, luminescence

Toward developing super-broadband LEDs using NIR phosphors, the effect of Ca substitution on the luminescence of Cr-doped $Y_3Sc_2Ga_3O_{12}$ garnet (YSGG) was evaluated. The valence of chromium ions in YSGG mainly takes two states, trivalent and tetravalent, and YSGG shows luminescence peaks at 740 nm (Cr^{3+}) in octahedral Sc sites and at 1530 nm (Cr^{4+}) in distorted tetrahedral Ga sites. The garnet host is very suitable for optical-sensing LED applications because these two emission bands closely match two NIR windows, NIR-I (600–950 nm) and NIR-III (1500–1800 nm), which are applied for bio-imaging. In this study, we demonstrated that the Cr^{4+} broad emission was improved by Ca substitution to control the photophysical properties. We concluded that YSGG:Cr^{4+} with D_{2d} symmetry in a unique distorted tetrahedron is a promising NIR phosphor for light-emitting applications.

1. Introduction

Optical sensing technology using the NIR band (i.e., 800–2500 nm) as a probe light is a useful measurement method that can detect trace amounts of chemical substances in a non-destructive and non-contact manner. Currently, halogen lamps (thermal light sources) and monochromatic LEDs are used as light sources. However, in recent years, phosphor-converted NIR-LEDs have attracted much attention as compact and reasonably priced NIR broad light sources.[(1)] Generally, the wavelength ranges required for sensing light sources have high transparency for bio-window regions: NIR-I (600–950 nm), NIR-II (1000–1350 nm), and NIR-III (1500–1800 nm). In addition, the light components corresponding to the high-sensitivity ranges of Si photodiodes (600–1100 nm) and InGaAs photodiodes (1300–1700 nm) are required.[(2)] Thus,

*Corresponding author: e-mail: NAKANISHI.Takayuki@nims.go.jp
https://doi.org/10.18494/SAM.2021.3320

ISSN 0914-4935

a phosphor-converting broadband NIR photodiode (1300–1700 nm) is also required.(2) Therefore, phosphor-converting broadband NIR-LEDs, which can be free spectral designs employing phosphors, will play a critical role in next-generation sensing light sources.

Among the various NIR luminescent materials, Cr-doped garnet ($\{A\}_3[B]_2(C)_3O_{12}$) crystals are the most important candidates for practical phosphors that exhibit broad NIR emission [the fundamental structure is shown in Fig. 1(a)]. In general, chromium (Cr) is stabilized in a trivalent state at the octahedral B sites in a regular garnet crystal. The photoluminescence is based on the d^3 system, with line emissions and/or broad emissions in the wavelength range of 650–950 nm, with the wavelength strongly depending on the crystal field.(3) On the other hand, Cr^{4+} (d^2 system) in the garnet structure is mainly located at distorted tetrahedral C sites (D_{2d} symmetry) [Fig. 1(b)]. The Cr^{4+} emission peak in garnet crystals is located between 1300 and 2000 nm,(4) which is a longer wavelength (lower energy) than that of Cr^{4+} in other crystal systems (900–1400 nm).(5) These two emission bands correspond to the bio-windows. In particular, broad PL emission from 1350 to 1800 nm corresponding to NIR-III is strongly required for the realization of broadband NIR-LEDs. However, the stable valence of Cr ions is usually the trivalent state; thus, charge compensation is required to produce tetravalent chromium.

In this study, to control Cr^{3+}/Cr^{4+} NIR emission in garnet crystal, we focused on the effect of substituting divalent Ca ions as a charge compensator on its photophysical properties. Herein, we report the photophysical properties of Ca^{2+}-doped $Y_3Sc_2Ga_3O_{12}:Cr^{4+}$ toward realizing a compact sensing light source using NIR phosphors. These results should be a significant contribution to the fields of inorganic chemistry and basic material engineering.

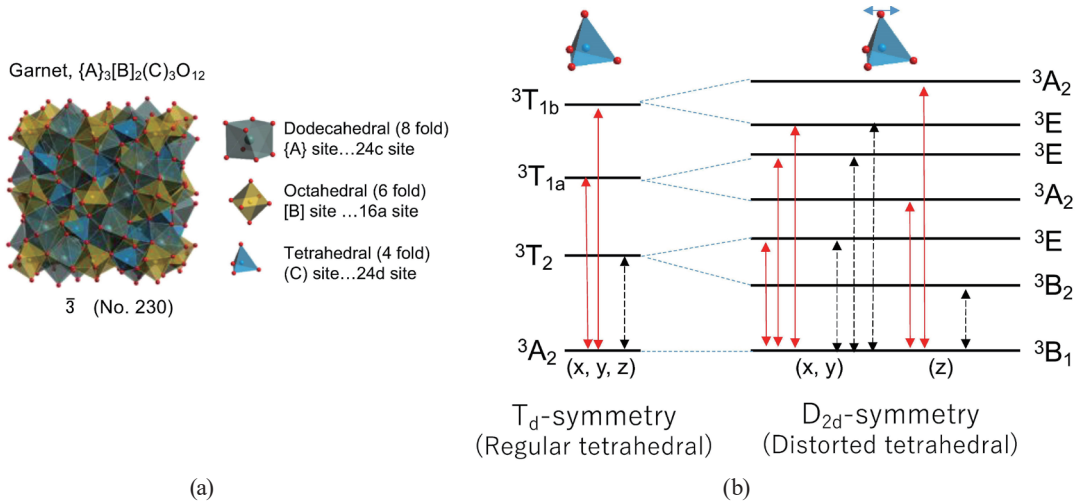

Fig. 1. (Color online) (a) Garnet structure: $\{A\}_3[B]_2(C)_3O_{12}$. A, B, and C donate different lattice sites with respect to their oxygen coordination: dodecahedral ($CN = 8$), octahedral ($CN = 6$), and tetrahedral ($CN = 4$), respectively. (b) Energy levels of tetrahedral Cr^{4+} (d^2) with *Td* symmetry (regular tetrahedron) and D_{2d} symmetry (tetragonal distorted tetrahedron). Red solid arrows are allowed electric dipole transitions and dashed black arrows are allowed magnetic dipole transitions.

2. Materials and Methods

2.1 Sample preparation

Cr^{3+}-Ca^{2+}-codoped YSGG ceramic samples with four different Ca^{2+} concentrations were fabricated by a conventional solid-state reaction. The compositions of the samples are listed in Table 1. Y_2O_3 (99.99%), Sc_2O_3 (99.99%), Ga_2O_3 (99.99%), $CaCO_3$ (99.9%), and Cr_2O_3 (99.9%) were used as raw materials. The starting powder was mixed by ball milling with anhydrous alcohol for 2 h. The mixed powder was dried at 60 °C for 24 h, compacted to form a ceramic green body under uniaxial pressing of 15 MPa, and finally sintered at 1600 °C for 12 h in air. Post-annealing treatment was performed in air at 1200 °C for 20 h to stabilize the tetravalent state of Cr.

2.2 Characterization

The phase compositions of the as-prepared Cr-doped YSGG garnet ceramic samples were measured by powder X-ray diffraction (p-XRD; D8 Advance Discover, Bruker Co.) utilizing nickel-filtered Cu $K\alpha_1$ radiation (1.5406 Å). Rietveld refinement of the samples was carried out with PDXL software (Rigaku Co.). The diffuse reflectance spectra were measured by a spectrophotometer (V-670, JASCO) equipped with an integrating sphere. PL excitation (PLE) and PL spectra were measured at room temperature by a VIS-NIR spectrofluorometer (FP-8700, JASCO) and calibrated using a standard halogen lamp. The temperature dependence of PL was measured by an InGaAs spectrometer (NIR Quest+2.2, Ocean Optics) under excitation with a 655 nm semiconductor fiber laser (CPS650F, Thorlabs) using a sample stage with a temperature control system (Rh10002L, -190 to 600 °C, Rinkam).

3. Results and Discussion

3.1 Structural analysis of Ca-doped YSGG:Cr (Ca = 0.5, 1.0, 2.0, and 4.0 mol%)

Figure 2(a) shows the p-XRD patterns of the Ca-doped YSGG:Cr series, along with the standard patterns from ICPDS (No. 024-1246). p-XRD peaks were assigned to the pure YSGG garnet phase by comparison with the crystallographic data. There was no peak shift of the XRD pattern with the Ca content. The refinement of the crystal structure revealed that the garnet phase belonged to the cubic system and the space group was Ia3d. The lattice constant was

Table 1
Compositions of the samples.

Amount of substituted Ca	Composition
0.5 mol%	$Y_{2.995}Ca_{0.005}Sc_2Ga_{2.99}Cr_{0.01}O_{12}$
1.0 mol%	$Y_{2.99}Ca_{0.01}Sc_2Ga_{2.99}Cr_{0.01}O_{12}$
2.0 mol%	$Y_{2.98}Ca_{0.02}Sc_2Ga_{2.99}Cr_{0.01}O_{12}$
4.0 mol%	$Y_{2.96}Ca_{0.04}Sc_2Ga_{2.99}Cr_{0.01}O_{12}$

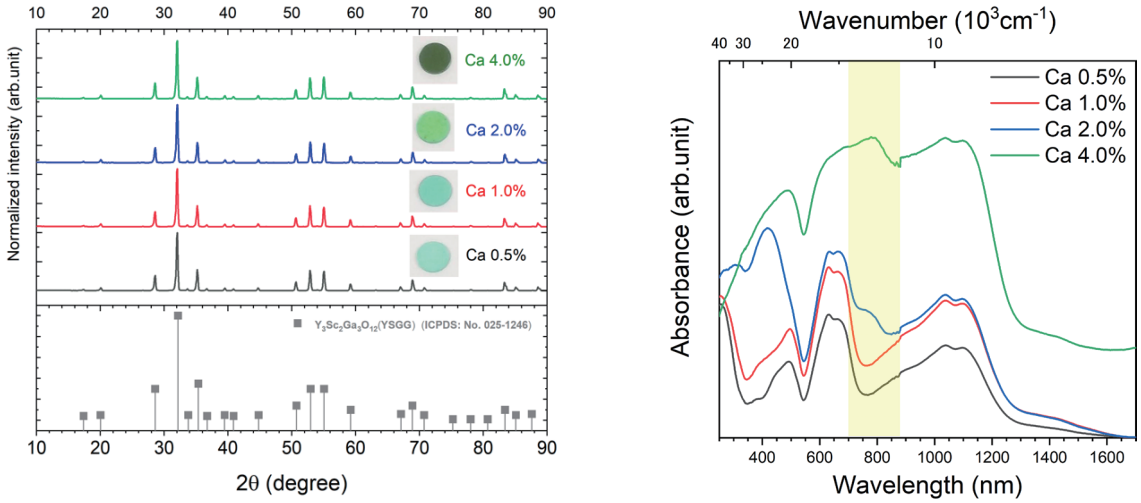

(a) (b)

Fig. 2. (Color online) (a) XRD patterns of Ca-doped YSGG:1.0 mol% Cr (Ca = 0.5, 1.0, 2.0, 4.0 mol%). Inset images are of as-prepared sample pellets. (b) Related absorption spectra (250–1700 nm).

calculated to be a = 1. 2481 nm (standard pure YSGG, a = 1.245 nm) for all samples. The reliability factor of the calculation was R_{wp} = 9.3%. As a result, we did not observe any change in the lattice constant upon calcium doping (Ca =0.5, 1.0, 2.0, 4.0 mol%). These results indicate that Ca (<4.0 mol%) is substituted at the dodecahedral yttrium sites because of their similar ionic radius and valence state in the garnet structure. In contrast, the sample color was clearly dependent on the Ca content (Fig. 2(a) inset). In this system, the predicted color center is only for Cr ions in these crystal fields. To identify the absorption centers, the diffuse reflectance spectra were measured, and estimated absorption spectra are shown in Fig. 2(b). The larger baseline of the sample with 4.0 mol% Ca is due to light scattering. A different absorption band at around 750 nm was observed in the samples with 2.0 and 4.0 mol% Ca. These absorption bands are attributed to regular $Cr^{3+}(d^3)$ in octahedral Sc sites (O_h) and $Cr^{4+}(d^2)$ in tetragonal Ga sites (distorted tetrahedra). Initially, we assumed that calcium only acted as a charge compensator for Cr^{4+} in Ga^{3+} sites; however, the existence of a new absorption band might indicate a valence change from Cr^{3+} to Cr^{4+} in garnet crystals.

3.2 Luminescence properties of Ca-doped YSGG:Cr

To clarify the effect of Ca substitution on the valence states of Cr ions, PL spectra of the samples excited at 510 nm were obtained, as shown in Fig. 3(a). Two broad emissions are observed at around 740 and 1530 nm. Unfortunately, our optical setup system using a cooling InGaAs detector could not monitor above a wavelength of 1650 nm, because it is outside the photodetector's sensitivity range. At a low Ca concentration (i.e., Ca = 0.5 mol%), the NIR emission in the 1530 nm band can hardly be observed. A marked increase in luminescence was observed upon increasing the Ca content to 1 mol%, equivalent to the amount of Cr. The emission spectrum with a peak at 740 nm is attributed to Cr^{3+},[(2)] and the emission at 1530 nm is

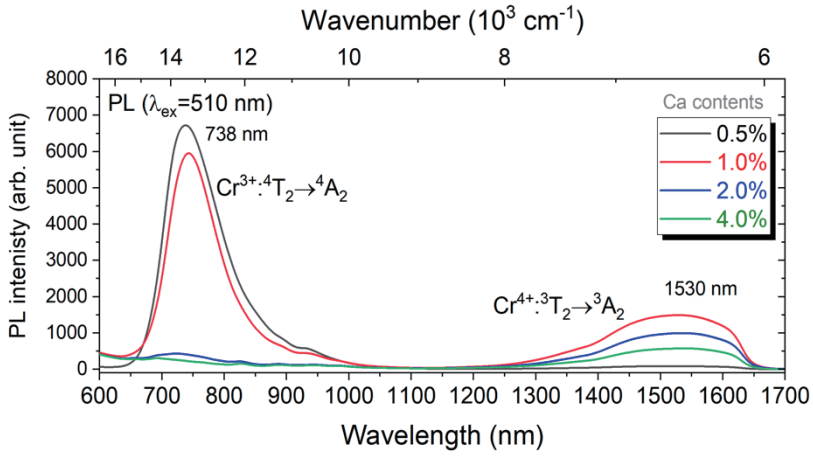

(a)

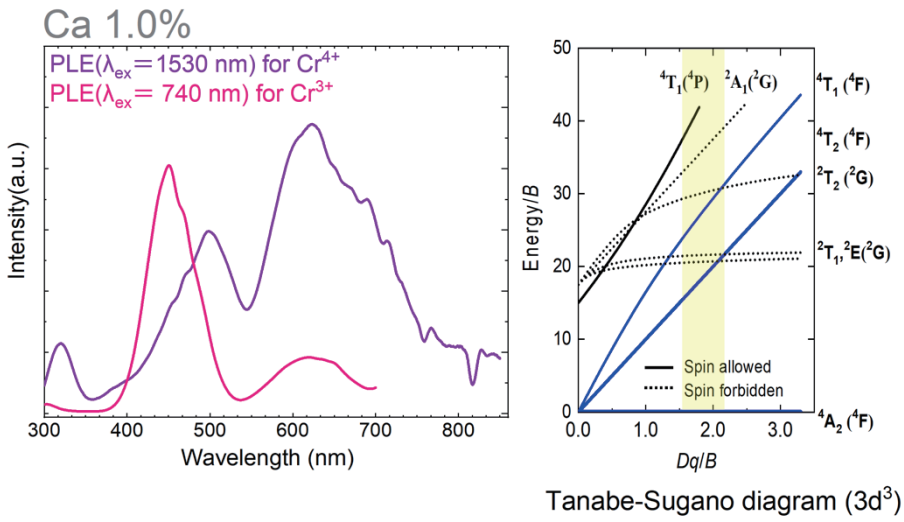

(b)

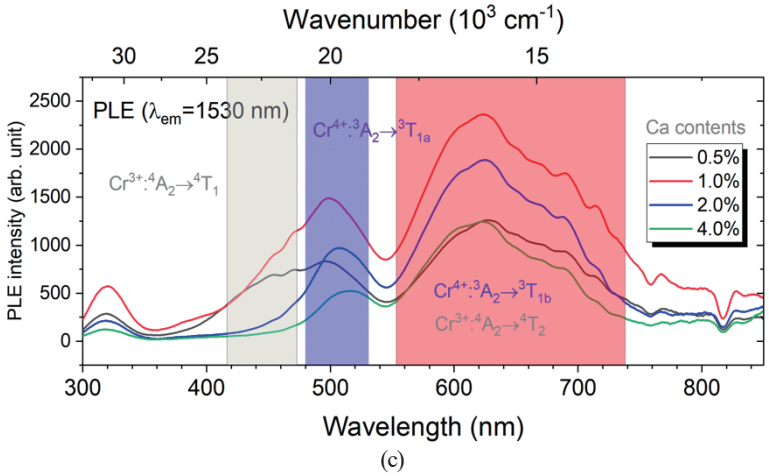

(c)

Fig. 3. (Color online) (a) PL spectra of all Ca-doped YSGG:Cr(1.0 mol%) samples, (b) PL excitation spectra of 1.0 mol% Ca-doped YSGG:Cr(1.0 mol%) monitored at 1530 and 740 nm. The right figure is the Tanabe–Sugano diagram of d^3, (c) PLE spectra of all Ca-doped YSGG:Cr(1.0 mol%) samples.

attributed to Cr^{4+} emission.(4) The PL intensity of Cr^{3+} decreased significantly with increasing amount of Ca, indicating that most of the Cr^{3+} changes to Cr^{4+} in this system upon Ca addition. Figure 3(b) shows the PLE spectrum of each sample over the range of emission wavelengths. The right of Fig. 3(b) shows the Tanabe–Sugano diagram of a typical d^3 electron system. Spin-allowed transitions from $^4A_2$ to $^4T_2$ (620 nm) and $^4T_1$ (460 nm) were observed by monitoring the 740 nm PL. On the other hand, it can be seen that the excitation spectrum of 1530 nm PL has different electronic transitions that partially overlap with Cr^{3+}. The spectrum had a complex shape with a fine structure, unlike the typical d^2 electronic transition with T_d symmetry. This is due to energy splitting by the distorted tetrahedron structure as shown in Fig. 1(b).

Figure 3(c) shows the PL excitation spectra for the samples with different Ca contents obtained by monitoring at 1530 nm. The spectral shapes were clearly different for the different samples, with a clearly observable band at 460 nm corresponding to the electronic transition of Cr^{3+}. It can be seen that the energy transfer from Cr^{3+} to Cr^{4+} contributes to the 1530 nm band emission. It was also found that the 1530 nm PL intensity changed with the Ca content and the intensity became maximum when the concentrations of Cr and Ca were equal (1.0 mol%). For the largest Ca content (4.0 mol%), the influence of Cr^{3+} was minimal judging from the intensity of the 460 nm absorption ($^4A_2$–$^4T_2$). The temperature dependence of the PL spectrum between 80 and 450 K is shown in Fig. 4. The spectral shape became asymmetric at low temperatures. Indeed, the zero-phonon line cannot be observed in this system at 80 K. Thus, we attributed the three PL emission bands at 1550, 1630, and 1750 to emissions from different tetragonal coordination sites. In fact, the scandium ions in $Y_3Sc_2Ga_3O_{12}$ ($\{A\}_3[B]_2(C)_3O_{12}$) can replace part of the A sites (mainly Sc in the B sites).(6) Therefore, there are multiple variations in the

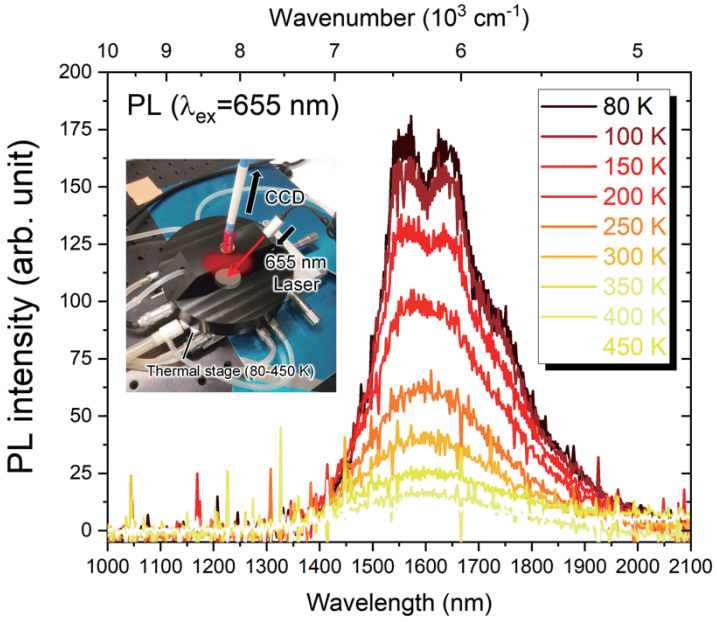

Fig. 4. (Color online) Temperature dependence of PL spectrum of Ca(1 mol%)-doped YSGG:Cr (80–450 K). The inset image is the measurement setup.

coordination environment of the C sites (Cr^{4+} replaced by tetrahedron), and the 1530 nm band emission has a broader shape at a lower energy.

Figure 5 shows the emission spectra of the samples after post-annealing at 1200 °C for 24 h. No significant change in the 1530 nm PL intensity was observed in the Ca = 1.0 mol% sample after annealing. When the Ca concentration was 2.0 or 4.0 mol%, i.e., higher than the Cr concentration (1.0 mol%), the PL intensity increased after annealing. Cr ions can be respectively substituted as Cr^{3+} and Cr^{4+} in the B and C sites of crystals.(4) Cr^{4+} in the C sites contributes to 1530 nm emissions; however, it is considered that there are many non-radiative transitions because no charge compensation occurs around Cr^{4+} in Ga^{3+}. Therefore, an equimolar amount of Ca is thought to replace the A sites to satisfy the local charge neutrality around Cr^{4+}, and the amount of active luminescent Cr^{4+} is increased to increase the PL intensity.

In addition, a new absorption band is also observed in the spectrum in Fig. 2(b). We speculated that charge compensation by calcium substitution not only contributes to the activation of luminescent species, but also induces changes in the valence of Cr ions. It is considered that the charge-compensated calcium was equilibrium diffused around the Cr^{4+} coordination geometry by post-heat-treatment. The tendency of increasing PL intensity at 1530 nm with increasing Ca concentration was stronger under this condition. We expect that the spectral design of chromium ions by the site engineering of garnets will be effective for the development of super-broadband LED light sources using combinations of NIR phosphors.

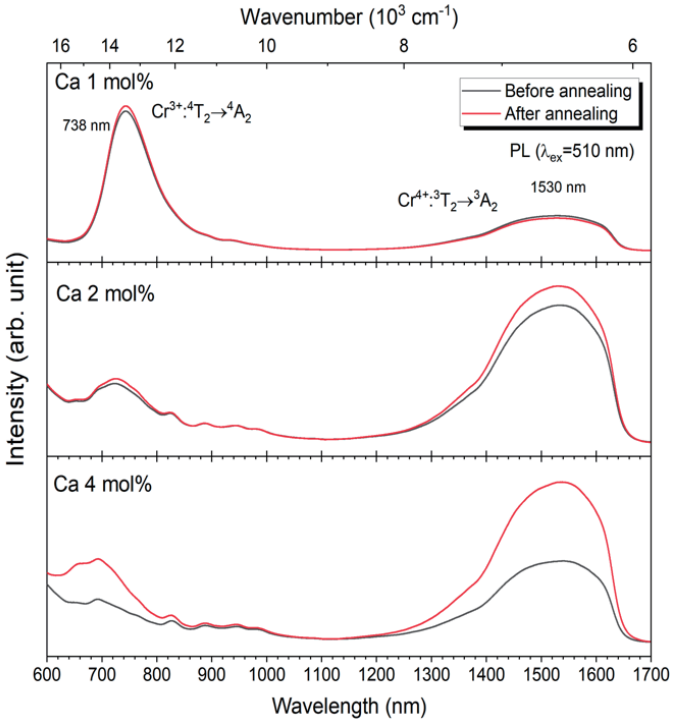

Fig. 5. (Color online) Effect of post-annealing of Ca-doped YSGG:Cr with 1.0, 2.0, and 4.0 mol% Ca. (a) PL spectra between 600 and 1700 nm upon excitation at 510 nm are shown.

4. Conclusions

In this study, the effect of Ca substitution on the photophysical properties of Cr-doped YSGG, which are strongly related to its valence states, was presented and analyzed. The Cr^{4+}/Ga^{3+} in the $Y_3Sc_2Ga_3O_{12}$ garnet structure was stabilized by the surrounding Ca^{2+}/Y^{3+} and showed an intense PL peak at 1530 nm because of charge compensation around chromium ions in distorted tetrahedral Ga sites. The two-emission balance of Cr^{3+} (at 740 nm) and Cr^{4+} (1540 nm) can be controlled by post-annealing. At the high Ca concentration of 4.0 mol%, the Cr^{4+} emission intensity was larger than that of Cr^{3+} in the garnet crystal, and the post-annealing treatment was more effective at a higher Ca concentration (>1.0 mol%). We expect that the spectral design of Cr ions by the site engineering of garnets will promote the development of super-broadband LED light sources using NIR phosphor combinations.

Acknowledgments

This research was financially assisted by the Sensor and Actuator R&D Project of National Institute for Materials Science (NIMS). This work was partially supported by Grant-in-Aid for Grant Number 17H04873.

References

1 M. Fang, P. Huang, Z. Bao, N. Majewska, T. Lesniewsk, S. Mahlik, M. Grinberg, G. Leniec, S. M. Kacznarek, C. Yang, K. Lu, H. Sheu, and R. Liu: Chem. Mater. **32** (2020) 2166. https://doi.org/10.1021/acs.chemmater.0c00101
2 J. Xu, D. Murata, J. Ueda, B. Viana, and S. Tanabe: Inorg. Chem. **57** (2018) 5194. https://doi.org/10.1021/acs.inorgchem.8b00218
3 Z. Jia, C. Yuan, R. Li, P. Sun, R. Dong, Y. Liu, L. Wang, H. Jiang, and J. Jiang: Phys. Chem. Chem. Phys. **22** (2020) 10343. https://doi.org/10.1039/C9CP03426A
4 S. Kück, K. Petermann, U. Pohlmann, and G. Huber: Phys. Rev. B **51** (1995) 17323. https://doi.org/10.1103/PhysRevB.51.17323
5 Y. Zhuang, S. Tanabe, and J. Qiu: J. Am. Ceam. Soc. **97** (2014) 3519. https://doi.org/10.1111/jace.13128
6 ICSD 39834. Reference is originated by V. A. Efremov, N. D. Zakharov, G. M. Kuz'micheva, B. V. Mukhin, V. V. Chernyshev, Zhurnal Neorganicheskoi Khimii' 1993 38 220 225.